

A Stretchable Ionic Diode from Copolyelectrolyte Hydrogels with Methacrylated Polysaccharides

Hae-Ryung Lee, Jaesung Woo, Seok Hee Han, Seung-Min Lim, Sungsoo Lim, Yong-Woo Kang, Won Jun Song, Jae-Man Park, Taek Dong Chung, Young-Chang Joo, and Jeong-Yun Sun*

As the demand for soft and flexible devices steadily increases, the ionic applications demonstrated with gel materials have come under the spotlight. Here, stretchable and wearable ionic diodes (SIDs) made from polyelectrolyte hydrogels are introduced. Polyelectrolyte hydrogels are mechanically modified using methacrylated polysaccharides while preserving the ion-permselectivity of poly(sulfopropyl acrylate) potassium salt (PSPA) and poly([acrylamidopropyl] trimethylammonium chloride) (PDMAPAA-Q), forming ionic copolymers. Then, SIDs composed of polyelectrolyte copolymer hydrogels are fabricated in VHB substrates as a stretchable and transparent insulating layer which is engraved by a laser. The SIDs show rectifying behaviors beyond the stretch of 3 with the aid of perfect adhesion between hydrogels and elastomeric substrates, and preserve their rectifications over hundreds of cycles. The operation of the SID is visualized by a wearable ionic circuit which rectifies ionic currents and lightens the LED under the forward bias during finger movements.

ion transports instead of electrons, have been demonstrated with soft materials including hydrogels and elastomers for wearable and pliable applications, for example, in pressure and stretch sensors on human skins^[1] and in ionic touch panels^[2,3] as input devices, as well as in a transparent ionic speaker,^[4] in flexible and wearable triboelectric nanogenerators,^[5,6] and an ionic power source^[7] as output devices. For operational or logic units, studies on ionic active circuit elements such as ionic diodes^[8–13] and transistors^[14–18] using ion-selective membranes or polyelectrolyte gels have been reported. In the case of polyelectrolyte (PE) hydrogels, charged polymeric chains form 3D networks, imbibing solvent molecules, in this case, water. PE gels have been usually

studied for mechanical enhancement of hydrogels,^[19–21] while ion-selectivity of PE hydrogels is another noticeable characteristic sought in ionic devices by researchers. The ion-selectivity of PE hydrogels comes from the fixed charges on the polyanionic or polycationic chains and their mobile counter ions present in order to satisfy charge neutrality. For example, cations are chiefly mobile, unlike anions in PE gels, which possess polyanionic networks due to Donnan equilibrium. Using the ion-selective properties of PE gels, ionic currents can be rectified in polyanionic and polycationic gel junctions under reverse bias. In addition, gels are intrinsically flexible and even stretchable materials, so they are advantageous for use in the production of wearable devices. Former studies on ionic circuit elements were focused on confirming the concept of ionic devices using brittle substrates^[9,10] or did not consider the issues associated with adhesion to flexible substrates which are necessary to wearable devices for insulations,^[8,13,22] thus, preventing them from being used in wearable products.


In this study, we propose stretchable ionic diodes (SIDs) with mechanically modified PE hydrogels. Ion-selective hydrogels with copolyelectrolyte chains were designed by mixing conventional charged monomers and methacrylated polysaccharides for SIDs. Then, SIDs were fabricated in stretchable and transparent elastomeric substrates. The SIDs exhibited rectifying behaviors under uniaxial stretching and sustained their performance at repetitive deformations.

1. Introduction

Following the development of more flexible and softer devices used in external areas of the human bodies, wearable ionic devices^[1–6] have drawn attentions to promptly meet the demands for the times. Ionic devices, operated by

H.-R. Lee, J. Woo, S.-M. Lim, S. Lim, Y.-W. Kang, W. J. Song, J.-M. Park, Prof. Y.-C. Joo, J.-Y. Sun
Department of Materials Science and Engineering
Seoul National University
Seoul 08826, South Korea
E-mail: jysun@snu.ac.kr

H.-R. Lee, J. Woo, S.-M. Lim, S. Lim, Y.-W. Kang, W. J. Song, J.-M. Park, Prof. Y.-C. Joo, J.-Y. Sun
Research Institute of Advanced Materials (RIAM)
Seoul National University
Seoul 08826, South Korea
S. H. Han, Prof. T. D. Chung
Department of Chemistry
Seoul National University
Seoul 08826, South Korea
Prof. T. D. Chung
Advanced Institutes of Convergence Technology
Suwon-Si 16229, Gyeonggi-do, South Korea

 The ORCID identification number(s) for the author(s) of this article can be found under <https://doi.org/10.1002/adfm.201806909>.

DOI: 10.1002/adfm.201806909

2. Results and Discussion

In this paper, we defined some terms associated with PE hydrogels to promote understanding. If a PE gel has polyanionic backbones with mobile cations as counter ions, it is called a p-type PE gel. In case of a PE gel with polycationic chains and mobile anions, it is called an n-type PE gel. When applying PE gels to ionic diodes, the application of as many monomers as possible is preferred to densify the charged networks of the PE gels, maximizing their ion-selective properties. However, the concentration of counter ions also increases to a higher proportion in monomers. Thus, PE gels undergo dramatic swelling due to the high osmotic pressure, and mechanical degenerations at the ends.^[23–26] When synthesizing highly concentrated PE gels, a significant amount of crosslinkers can reduce the degree of swelling, but a high crosslinking density of gel networks results in brittle materials. To obtain PE gels with a high ion-selectivity and fair mechanical properties for the manufacturing of the SIDs, two types of PE hydrogels have been modified by using polysaccharide chains, generating polyelectrolyte copolymers (Figure 1). For p-type PE gels, 3-sulfopropyl acrylate potassium salt (SPA) which provides fixed negative charges from sulfonate groups in polymeric backbones along with mobile potassium ions was selected as a monomer. Treated by glycidyl methacrylate, hyaluronic acid with carboxylic functional groups (GM-HA)

was added as an intensifier to modify poly(3-sulfopropyl acrylate) (PSPA) gels (Figure 1a,b). 3-acrylamidopropyl[trimethylammonium] chloride (DMPAA-Q) that has fixed positive charges from ammonium groups in polymer chains along with mobile chloride ions was used as a monomer in n-type PE gels. Methacrylated chitosan (GM-CTS) also with ammonium functional groups was adopted as n-type PE gel reinforcing agents (Figure 1c,d). While SPA and DMAPAA-Q form short chains with the crosslinking agent of *N,N'*-methylenebisacrylamide (MBAAm), methacrylated polysaccharide materials provide relatively long chains, favorable to chain entanglements. The monomers (SPA and DMAPAA-Q) can be crosslinked by both MBAAm and methacrylated polysaccharides (GM-HA and GM-CTS), generating PE copolymer gels. Since carboxyl groups in GM-HA can be negatively charged in aqueous conditions, cations are still able to pass through the two types of polyanionic networks (PSPA and GM-HA), while anions are blocked as shown in Figure 1a,b. In a similar mechanism, ammonium groups in GM-CTS allow the transport of anions while interrupting that of cations via polycationic chains of poly(3-acrylamidopropyl[trimethylammonium] chloride) (PDMAPAA-Q) in n-type PE copolymer gels. Details for the synthesis of PE copolymer gels are described in the Experimental Section.

To demonstrate and analyse the electrical properties of PE hydrogels using numerical data, a salt bridge model, which

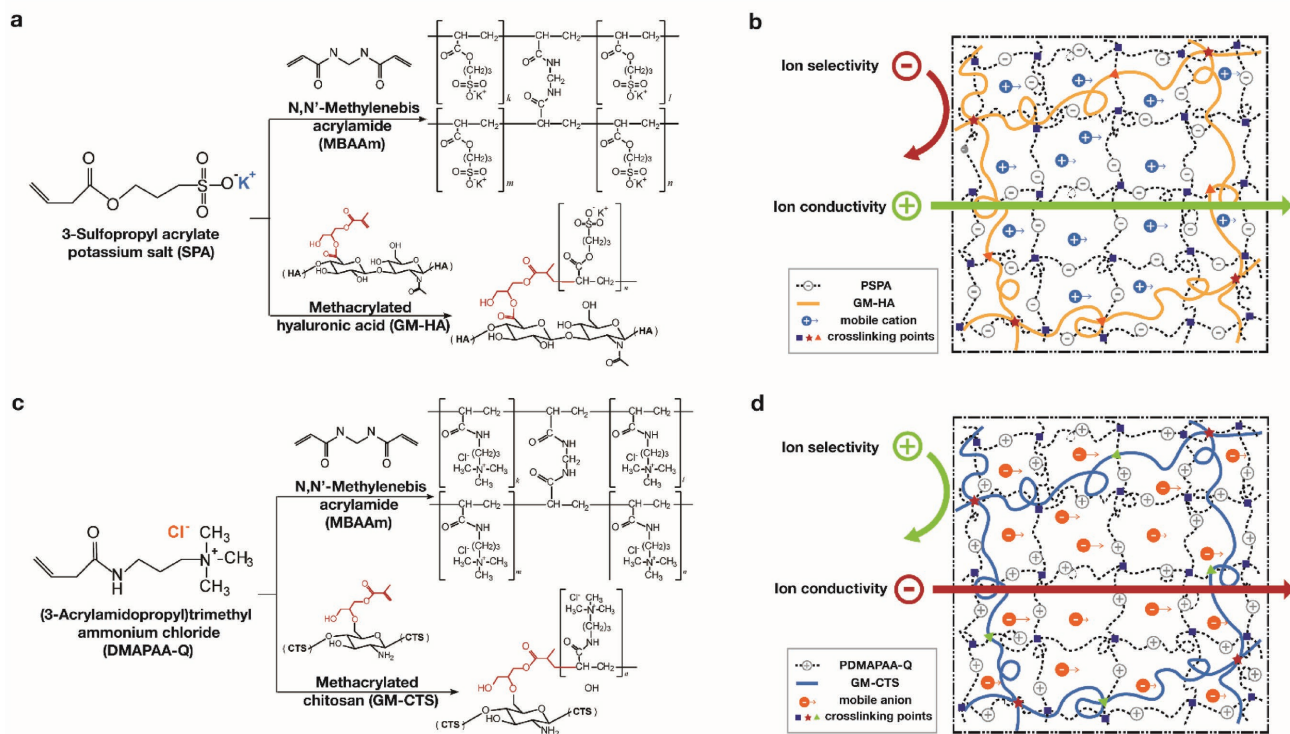


Figure 1. Modulation of polyelectrolyte gels by the addition of methacrylated polysaccharides. To generate SIDs, two types of PE gels have been modified using polysaccharide chains with methacrylate functional groups. a, b) Chemical structures and the schematic illustration of PSPA crosslinked by MBAAm with methacrylated hyaluronic acid (GM-HA) as the p-type PE gel. Negatively charged sulfonate groups in the PSPA and charged carboxyl groups in the GM-HA interrupt the transport of anions (ion-selectivity of p-type PE gels) while allowing cations to pass through the copolyelectrolyte chains (ion-conductivity of p-type PE gels) due to the Donnan equilibrium. c, d) Chemical structures and the schematic illustration of PDMAPAA-Q crosslinked by MBAAm with GM-CTS as the n-type PE gel. Positively charged ammonium groups in PDMAPAA-Q and GM-CTS block cations (ion-selectivity of n-type PE gels) while enabling anions to be transported (ion-conductivity of n-type PE gels).

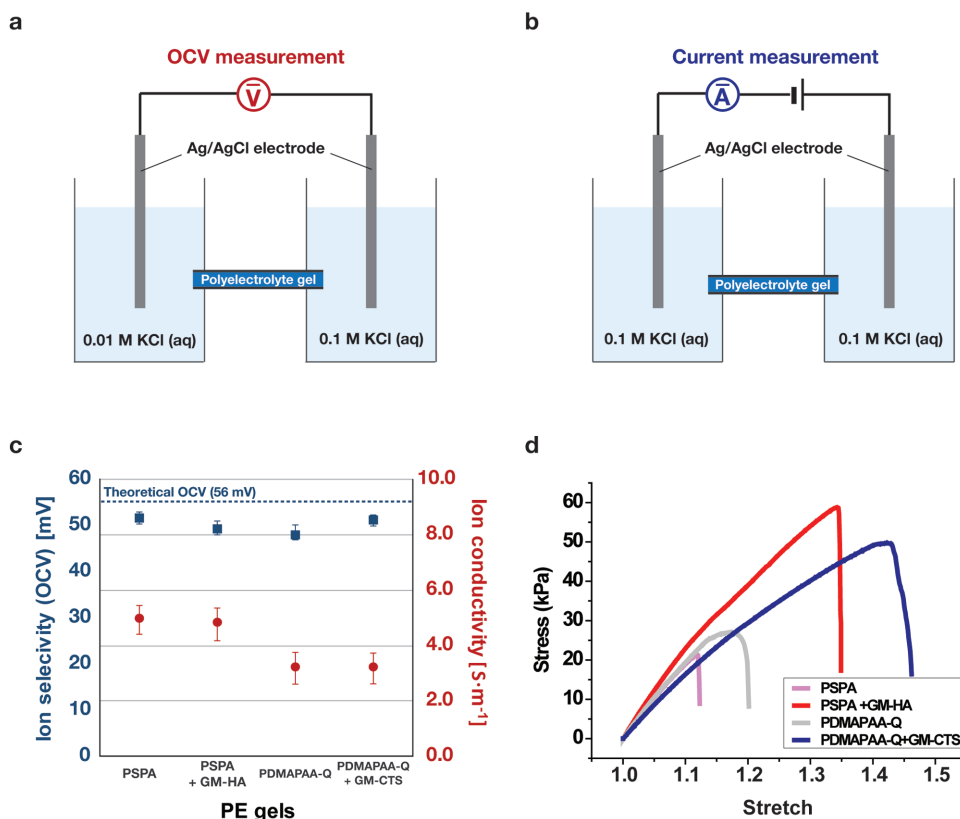


Figure 2. Electrical and mechanical properties of copolyelectrolyte hydrogels. a,b) Salt bridge models for measuring ion-selectivity and ion-conductivity of PE gels before and after modification. a) OCV between potassium chloride reservoirs with two different concentrations (0.01 and 0.1 M) were measured to define the ion-selectivity of the PE gel. Ion-selective materials exhibit OCV between two different concentrations according to the Nernst equation. b) An illustration of the salt bridge model for measuring ion-conductivity of PE gels. Two reservoirs were filled with KCl of the same concentration (0.1 M). c) Ion-selectivity and ion-conductivity values of PE gels before and after adding GM-HA and GM-CTS. Error bars show standard deviation; sample size $n = 3$. d) The stress–stretch curves for PE gels. PSPA and PDMAPAA-Q gels were too brittle to be handled at the macro scale. By adding 0.01 wt% of methacrylated polysaccharide material, the maximum stretch of both p- (PSPA + GM-HA) and n-type copolyelectrolyte hydrogels (PDMAPAA-Q + GM-CTS) was increased to 1.35 and 1.46, respectively.

consists of a PE gel sample placed between two electrolyte reservoirs, was adopted. Ion-selectivity and ion-conductivity of PE gels before and after the modifications were compared by measuring open circuit voltages (OCVs) and ionic currents of gel samples as described in **Figure 2a,b**. The OCV between the two reservoirs of different concentrations of potassium chloride (0.01 and 0.1 M) were measured to define the ion-selectivity of the PE gel. According to the Nernst equation, electrical potential can be generated by a concentration gradient

$$\Delta E = \frac{RT}{zF} \ln \frac{C_1}{C_2} \quad (1)$$

Assuming a PE gel with perfect ion-selectivity, only one type of ion is able to diffuse from a highly concentrated reservoir to a reservoir with a low concentration. In this case, the theoretical value of the OCV is 56 mV. In case of polyelectrolyte gels with less ion-selectivity, both cations and anions can infiltrate into the gels and OCV values less than 56 mV are obtained. If the material has no ion-selectivity, the OCV drops to zero. **Figure 2b** describes the experimental setup for measuring the ion-conductivity of PE gels. The currents running through the PE gels placed between two KCl reservoirs with the same

concentration of 0.1 M was measured. In the case of p-type PE gels, the ion-selectivity of the modified PE gel (PSPA + GM-HA) decreased compared to that of the unmodified single-networked gel (PSPA), but the decrement was less than 4% which was not sufficient to prohibit for the p-type copolyelectrolyte hydrogels from being used as ion-selective materials. The n-type copolyelectrolyte hydrogel (PDMAPAA-Q + GM-CTS) showed better ion-selectivity than that of the unmodified gel (PDMAPAA-Q). Additionally, the ion-conductivity in both p- and n-type copolyelectrolyte hydrogels were maintained constant (**Figure 2c**). Tensile tests were also conducted to confirm the mechanical properties of the PE gels before and after modification. Before modification, the highly concentrated PSPA and the PDMAPAA-Q gels were too brittle to be handled on macro scales. By adding 0.01 wt% of methacrylated polysaccharide materials, the maximum stretch of both p- (PSPA + GM-HA) and n-type copolyelectrolyte gels (PDMAPAA-Q + GM-CTS) was increased from 1.125 to 1.35, and from 1.2 to 1.46, respectively.

With the interpenetrating PE gels, the SIDs were fabricated in a VHB substrate, which is transparent, highly stretchable, and attachable. In **Figure 3a**, VHB substrates with triangular microchannels were prepared by laser engraving to wrap the gel parts of the ionic diodes. The triangular design was

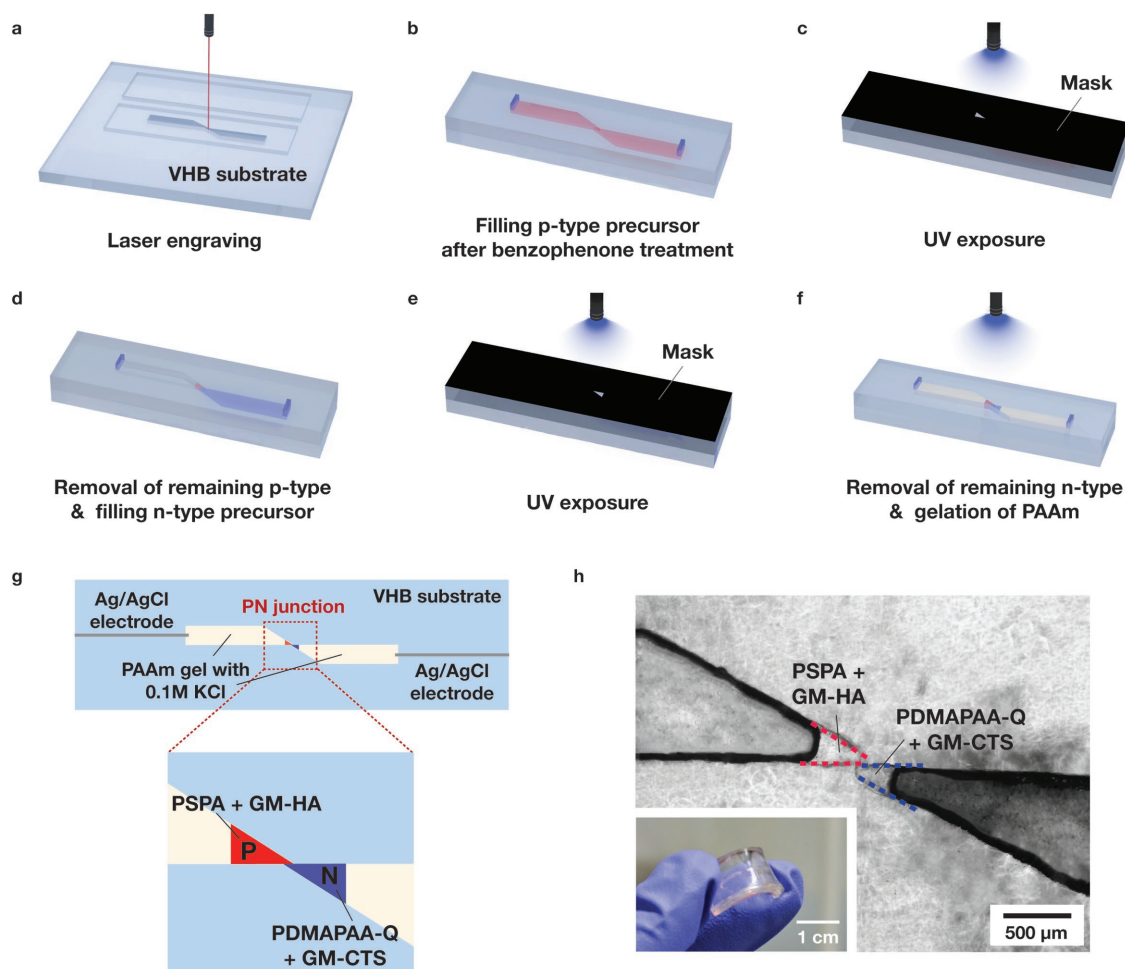


Figure 3. Fabrication of SIDs in VHB by laser engraving. a) Triangular microchannels were engraved in VHB by a laser. b) A VHB substrate with an engraved channel was attached to a VHB cover with holes necessary for injecting and extracting the precursor solutions of the PE gels. After preparing the diode frame, the channel was treated with benzophenone to generate chemical adhesions between the PE gels and the VHB. The p-type precursor solution was filled into the channel. c) With a patterned UV mask, the p-type PE gel was crosslinked on a single side of the channel under the exposure of UV light of 365 nm for 10 s. d) Removing the unreacted precursor solution of the p-type gel, the n-type precursor solution was filled. e) The n-type PE gel was synthesized beside the p-type gel with the same method, resulting in a P–N junction. f) Eliminating the remainder of the n-type precursor, polyacrylamide gels with potassium chloride salts were made, filling the rest of the engraved channel. g) A planar view of a SID. The P–N junction by PE gels is in the middle of the ionic diode, and the electrolyte reservoir made by PAAm gels with potassium chloride solutions connects the PE gels to the Ag/AgCl electrode. h) An optical microscope image of the P–N junction by PE gels in a VHB substrate. The subset image shows the entire appearance of the SID after the procedure from (a) to (e).

intended to narrow down the P–N junction area.^[9] This areal gradient induced a bottleneck effect, minimizing the cross-sectional area of the P–N junction compared to other gel parts. Thus, the potential drop was intensified at the middle of the P–N junction and the measurability ionic currents at the P–N junction was raised up. Since we are able to adjust the power and speed of the laser beam, the fabrication of microchannels with diverse shapes and dimensions was simple, requiring only tens of seconds. Then, the engraved VHB was covered with another VHB layer containing holes, necessary for the injection and extraction of the precursor solutions of the PE gels. After preparing the diode frame, the channel was treated by benzophenone to induce chemical adhesions between PE gels and the VHB.^[27] The channel was filled with the precursor solution of PSPA modified with GM-HA (Figure 3b). Using a patterned UV-resistant film above the VHB frame, the p-type

copolyelectrolyte hydrogel was synthesized on a single side of the channel under the exposure of UV light (365 nm) for 10 s (Figure 3c). After removing the unreacted precursor solution of the p-type gel, the precursor solution for the n-type copolyelectrolyte hydrogel was filled in. The n-type copolyelectrolyte gel was synthesized next to the p-type gel using the same method (Figure 3d,e), generating a P–N gel junction in the middle of the ionic device. Electrolyte reservoirs made by polyacrylamide (PAAm) gels with KCl solutions were synthesized after the P–N junction was made (Figure 3f,g), thus spacing the polyelectrolyte copolymer gels and the Ag/AgCl electrodes to prevent a large potential drop at the direct interface of the PE gel and the electrode.^[9] The height and length of the PE gels were 270 and 300 μm, respectively. The intersection of the P–N junction was 80 μm. We could confirm the formation of the P–N junction with a clear boundary between the p- (left

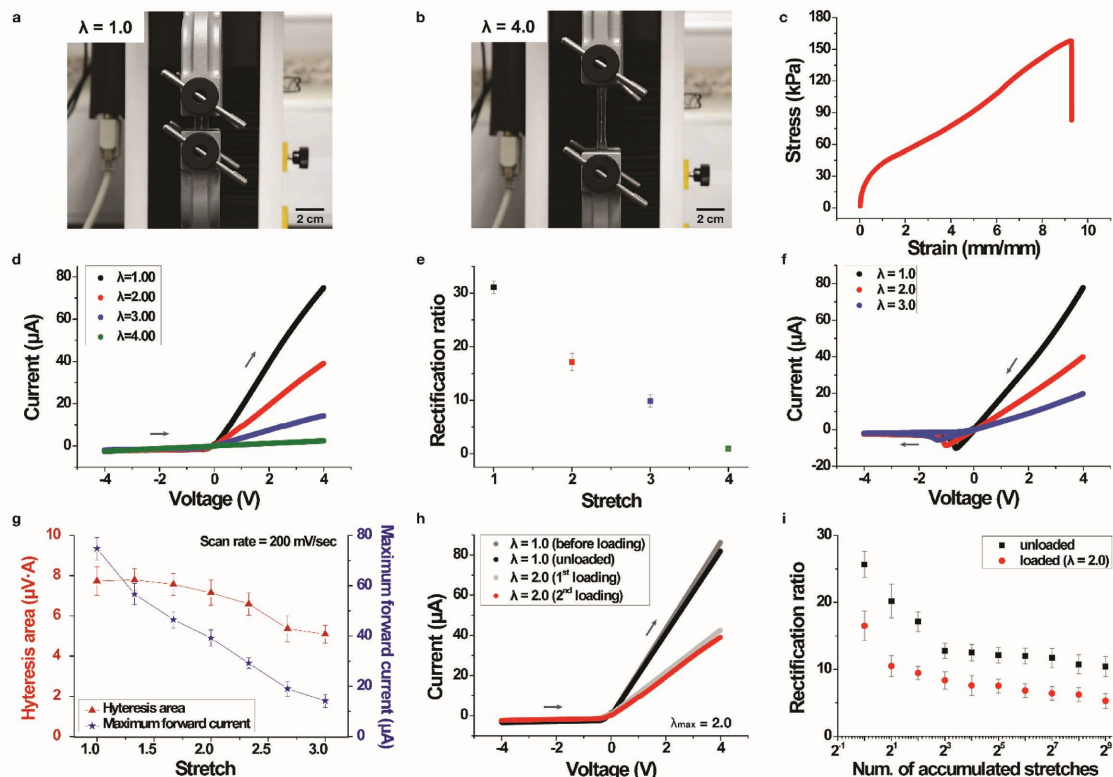


Figure 4. Rectification behaviors of SIDs under applied strains. a, b) A SID before and after stretch of up to 4. c) A stress–strain curve of SID in VHB. The maximum stretch of the SID was 9 since the copolyelectrolyte gels and VHB formed perfect adhesion. d) The current–voltage responses of a SID were measured through a forward scan ranging from -4 to 4 V. The scan rate was 200 mV s^{-1} . e) The rectification ratio under the various stretches. The rectification ratio is the maximum current at 4 V divided by the minimum current at -4 V. Error bars show standard deviation; sample size $n = 3$. f) Electrical properties of SIDs measured by a reverse scan from 4 to -4 V. Hysteresis in an I – V sweep was observed due to the presence of residual ions at the P–N junction which were stored by the forward bias. g) The hysteresis area of the I – V curves in (f) was integrated to determine the quantity of residual ions in the P–N junction. Error bars show standard deviation; sample size $n = 3$. h) Rectification of a SID was confirmed for cyclic loadings. The maximum stretch was fixed at $\lambda_{\text{max}} = 2$. i) The rectification ratio of SIDs measured for 500 cycles. A maximum stretch of $\lambda_{\text{max}} = 2$ was applied for all cycles. Owing to the viscoelastic properties of VHB substrates, the SIDs sagged to $\approx 12.5\%$ of their initial length after the SIDs were unloaded from the 400th cycle. Error bars show standard deviation; sample size $n = 3$.

and n-type (right) PE gels (Figure 3h). The subset in Figure 3h is the entire appearance of the SID after the procedure from Figure 3a–e. The white scale bar indicates 10 mm.

The SID seemed to be stretched over nine times its original length due to the high stretchability of the VHB substrate, which occupied the majority of the wearable device (Figure 4c). However, when the electrical properties of the SIDs were measured by voltage sweep and cyclic voltammetry tests, the SIDs that stretched to more than quadruple their original length were rather ionic conductors, not ionic diodes (Figure 4d). According to the I – V curves of the SID under stretches in Figure 4d, rectification of ionic currents under the reverse bias was observed up to stretch of 3, while a linear increase in current was noted under the forward bias. The increased stretchability of the SID compared to free-standing copolyelectrolyte hydrogels was allowed due to strong chemical adhesion between the gel materials and the surface-treated elastomeric substrates, suppressing the strain localization in amorphous gels with initial flaws.^[28] The maximum current of the SID decreased as the applied strain was increased—the longer the SID, the higher its resistance was—while the reverse current was close to zero. The voltage sweep ranged from -4 to

4 V with a scan rate of 200 mV s^{-1} . In Figure 4e, the rectification ratio of the SID in Figure 4d was calculated using the ratio of the maximum current at 4 V divided by the minimum current at -4 V. The initial value of the SID with no applied strain was 31. The rectifying ability, represented by the rectification ratio, was diminished as the SID was stretched further because the maximum forward currents were directly influenced by increased resistances as more uniaxial elongations were applied while the maximum reverse currents, suppressed at the beginning, did not show noticeable variations along with stretches. When the electrical properties of the SIDs were measured by a reverse scan from 4 to -4 V, hysteresis of the SID was observed due to the presence of residual ions at the P–N junction during the forward bias (Figure 4f). The recovery of the rectified currents appeared later at a larger reverse bias as more stretch was applied. Delayed recoveries of ionic currents during the reverse bias under further stretching were caused by the extended length of the P–N junction. The area of hysteresis of the I – V curves during reverse bias in Figure 4f was integrated to determine the quantity of ionic charges passing through the P–N gel junction in Figure 4g. A larger hysteresis area reflects a larger flow of ionic current at lower loads during the previous forward

bias. The forward scan of the SIDs from -4 to 4 V before stretch and after a stretch of up to 2.0 was attempted to certify the durability of SIDs under repetitive stretches (Figure 4h,i). In Figure 4h, the first voltage scan from reverse to forward bias was done before loading ($\lambda = 1.0$); then, the sample was stretched to $\lambda = 2.0$. After measuring the I - V responses of the SID under $\lambda = 2.0$ (first loading), the applied load was removed, and the black curve, $\lambda = 1.0$ (unloading), was obtained. The red curve in Figure 4h, $\lambda = 2.0$ (second loading), was obtained after the second loading and stretching up to 2 . The initial trials for recovery confirmed a fair repeatability of the SID rectifying performance as shown in Figure 4h. Additional forward scans on the same SID sample from -4 to 4 V were explored under repetitive stretches of up to 2.0 over 500 times. The rectification ratio of the SIDs at no applied strain showed a convergence of ≈ 12 , while the same sample at a stretch of 2.0 resulted in ≈ 5 . Due to the viscoelastic property of the VHB substrate, the SIDs did not maintain their initial states in length after hundreds of stretches up to 2.0 . The SIDs were sagged about 12.5% of the initial state after the 400 th test cycle was completed, and the time-consuming recovery of the VHB substrate is thought to deteriorate rectifying performances of the SIDs after hundreds of cycles. Even though the applied stretch of 2 is a fairly harsh condition in daily lives, considering deformations in human bodies are possible about 1.4 at most, flexible ionic diodes with durability would be possible from less viscoelastic substrates like PDMS and Ecoflex.

The integration of SIDs with electrical circuit elements was available in fully wearable forms. To visualize the operation of SIDs under deformations, a wearable ionic circuit with two ionic diodes and two LEDs was demonstrated. The stretchable and wearable ionic circuit was designed as shown in Figure 5a. A yellow LED and a green LED with identical specifications (except for their colours) were connected separately to one SID each. The anodes of the two LEDs were positioned on the right, and the upper ionic diode was placed in the same direction as the LEDs while the lower one was in the opposite direction. A PAAm hydrogel with $\text{KCl } 2 \text{ M}$ was used as an ionic conductor. The wearable ionic circuit was attached to an index finger and operated by a DC voltage source. The positive terminal of

the power source was connected to the ionic diodes, and the negative terminal was connected to the anode of LEDs. When the finger was spread out and bent, only the yellow LED connected to the ionic diode in the same direction was turned on at a forward bias of 8 V . The brightness of the yellow LED was slightly lessened and a lower current was measured when the finger was bent (Figure 5b). Since metal wires from LEDs were remained to connect electrical components and ionic conductors, electrochemical reactions at the interface of LEDs and PAAm gels occurred. The performances of the SIDs in the wearable ionic circuit were sustainable despite the undesirable electrochemical reactions at the interface of metals and PAAm ionic conductors. The integration of SIDs with circuit elements like ionic power sources and soft input devices made by hydrogels are expected to be possible in further studies though we adopted lightening electrical circuit components to demonstrate the SID here.

3. Conclusion

SIDs and wearable ionic circuits were demonstrated by copoly-electrolyte hydrogels. Polysaccharides with methacrylate functional groups enhanced mechanical properties of conventional polyelectrolyte hydrogels and maintained the ion-selectivity and -conductivity for the SIDs and wearable ionic circuits. Insulating layers for wearable ionic diodes were adopted to avoid leakage currents. Chemical adhesions between solid-phase ionic materials including polyacrylamide gels and elastomeric substrates contributed to generate the SIDs by preventing further swelling of the polyelectrolyte gels. The SIDs rectified the ionic currents when stretched beyond four times their original length, and endured hundreds of cycles under the maximum stretch of up to 2 . An integration of the SIDs to wearable devices was demonstrated by fabricating a wearable circuit which operates during finger movements. Further integrations of SIDs with other circuit elements like ionic power sources, soft energy harvesting systems, and triboelectric generators are expected to be possible in future works. In addition, engraving elastomeric substrates by a laser was suggested as a new simple method to make wearable devices within tens of seconds, thus having a merit on mass production.

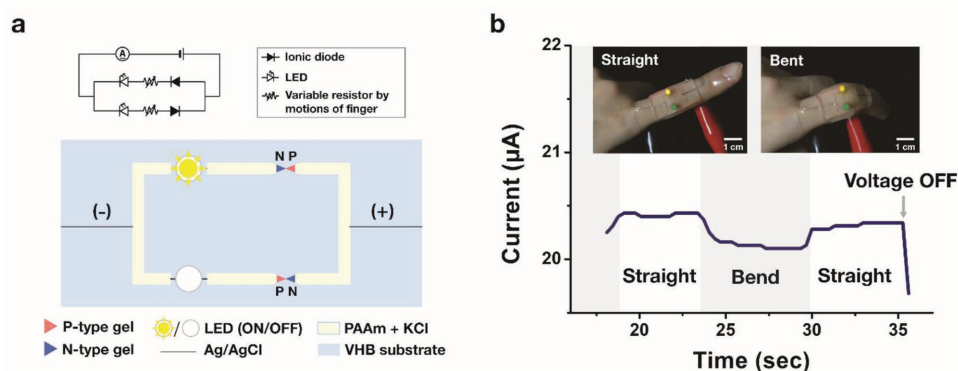


Figure 5. A wearable ionic circuit with SIDs and LEDs. a) A circuit diagram and a schematic illustration of the wearable ionic circuit. The LEDs placed in the same direction were connected to two oppositely positioned ionic diodes in a VHB substrate. VHB substrates were engraved by laser cutting system. A PAAm hydrogel with $\text{KCl } 2 \text{ M}$ was used as an ionic conductor. b) The wearable ionic circuit was worn on the finger, and the finger was spread out and bent. Only the yellow LED connected to the ionic diode in the same direction was turned on. The brightness of the yellow LED can be controlled by bending the finger.

4. Experimental Section

Synthesis of PSPA, PDMAPAA-Q, and Copolyelectrolyte Hydrogels: For nonmodified PE gels, SPA (251631 Aldrich) and DMAPAA-Q (448281 Aldrich) were chosen as p- and n-type monomers, respectively. The concentration of both types of monomers was 3 M. MBAAm (M7279 Sigma), consisting of 4 wt% of monomers, was used as a crosslinking agent. For copolyelectrolyte hydrogels, hyaluronic acid (average MW 2 000 000) was treated with glycidyl methacrylate (GM, 779342 Aldrich) to graft the methacrylate functional group.^[22] Chitosan was previously dissolved in a 0.4 M acetic acid solution and 0.05 M potassium hydroxide solution was added for a concentration of 5 wt% of the total mixture. Then, the chitosan aqueous solution was treated with GM using the same method as that used for GM-HA. The amount of GM-HA in the total p-type precursor solutions and GM-CTS in the total n-type precursor solutions were both 0.2 wt%. Lithium phenyl-2,4,6-trimethylbenzoylphosphine (LAP, 900889 Aldrich) was used as a photoinitiator. The amount of LAP was 0.0015 wt% of the total precursor gel solution.

Mechanical Tests on PE Gels: PE gel samples (made following the directions shown above) were prepared in 5 mm × 20 mm × 3 mm under UV light exposure for 30 min in a UV crosslinker (CL-1000L, UVP). Tensile tests were done by Instron (3343, Instron) with a load of 50 N. The tensile rate was 0.1 mm s⁻¹.

Ion-Selectivity and Ion-Conductivity Tests on PE Gels: To setup the salt bridges, PE gels were synthesized in glass tubes having a length of 5 cm and an inner diameter of 0.8 mm. To allow covalent bonds between the glass and the PE gel materials to prevent leakage currents, the glass tubes were washed in methanol and treated with 3-(trimethylsilyl) propyl methacrylate (TMSPMA, 0.01 wt% in methanol) for 2 h. Then, 0.01 and 0.1 M potassium chloride solutions were prepared for measuring the open circuit voltages, while 0.1 M potassium chloride solution was placed in both reservoirs to measure the ionic currents. An electrochemical analyser (MP3, ZIVE) and Ag/AgCl electrodes were used in these experiments. The number of samples was 3.

Fabrication of SIDs: VHB (4905, 3M) having a thickness of 500 μm was adopted as an elastomeric substrate to produce the SIDs. Three layers of VHB were prepared: a cover layer with two holes for injecting precursor solutions and extracting the remaining unreacted materials, a microchannel layer for the P–N junction and PAAm gel, and a bottom layer for packaging. It was not necessary to use a special treatment to attach these three layers since the substrate itself was an acrylic adhesive. A laser cutting machine (VLS 3.50, Universal Laser System) was used to produce the VHB substrates for the SIDs. Before gelation, the microchannel for the ionic diode was treated with benzophenone (10 wt% in ethanol) for 5 min.^[21] After washing off the treated microchannel with ethanol, the precursor solution for the p-type copolyelectrolyte gel was injected with a pico-injecting system (PLI-100A Delux, WARNERS INSTRUMENT). The sample was arranged and covered with a patterned UV resistive film by inverted microscopy (CKX41-A32PH standard, Olympus Korea), and exposed to 365 nm UV light to synthesize the p-type copolyelectrolyte hydrogel by a UV lamp light guide (BW 200 V3.0, DYMEX) for 10 s. With the same method, the n-type copolyelectrolyte gel was synthesized in the middle of the microchannel (beside the p-type gel) after sucking the unreacted p-type gel precursor solutions using a pico-injector. The dimensions of a single triangular gel plug were 300 μm × 270 μm × 500 μm. The area of the P–N junction was 80 μm × 500 μm. The surface power density of the UV light was 8–12 W cm⁻². After generating the P–N gel junction, polyacrylamide gels with 0.1 M of potassium chloride salts were synthesized, filling in the remaining area of the inner channel. 1.5 wt% of acrylamide (AAM, A8887, Sigma-Aldrich), 0.0078 wt% of MBAAm and 0.004 wt% of LAP were mixed to synthesize the PAAm gel for the neutral ionic conductor. PAAm gels were made under a UV crosslinking chamber (CL-1000L, UVP) for 30 min.

Tensile Tests on SIDs: The initial dimensions of a SID sample were 10 mm × 20 mm × 1.5 mm. Adopting jaw phases with acrylic plates (10 mm × 40 mm × 1 mm) to the SID, the initial length of the test sample was 10 mm. Tensile tests were conducted using Instron (3343, Instron)

with a load of 1 kN. The tensile rate was 0.1 mm s⁻¹. The number of test samples was 3.

Voltage Sweep and Cyclic Voltammetry on SIDs: The SIDs were washed off by KCl 0.1 M solutions overnight. Before measuring the electrical properties of SIDs, a reverse voltage (−4 V) was applied to them for 3 min with platinum electrodes to remove remnant materials left over from gel synthesis. When measuring the electrical behaviour of the SIDs, Ag/AgCl electrodes were used. The range of voltage sweep was from −4 to 4 V, while cyclic voltammetry was conducted from 4 to −4 V and from −4 to 0 V. There was no lag time when switching the direction of the applied bias. The scan rate was 200 mV s⁻¹. An electrochemical analyser (MP3, ZIVE) and potentiostat (Reference 600+, Gamry) were used to explore the rectifying behaviours of the SIDs.

Cyclic Tests on SIDs: For cyclic tests, the initial length of the SID was 6 mm (excluding some of PAAm parts and Ag/AgCl electrodes). The SIDs were positioned on the hand-made stretcher and stretched up to 12 mm, and then, the applied strain was immediately removed. The stretch rate was 6 mm s⁻¹.

Fabrication and Operation of the Wearable Ionic Circuit with SIDs: The overall mechanism to fabricate the wearable ionic circuit was similar to the one employed to manufacture the SIDs, using laser engraving of VHB and photopolymerization of copolyelectrolyte hydrogels, with the exception of the circuit design. Two LEDs were placed after the ionic diodes by the PN gel junctions and the ionic conductor (PAAm with KCl 2 M) parts were fully prepared. A DC voltage of 8 V was applied to the ionic circuit using a function generator (3361A, Agilent), and the currents were measured by a multimeter (34461A, Agilent).

Acknowledgements

This work was supported by Samsung Research Funding Center of Samsung Electronics under Project Number SRFC-MA1402-11. H.-R.L. was supported by Global Ph. D. Fellowship Program through the National Research Foundation of Korea (NRF) funded by the Ministry of Education (2015H1A2A1033235).

Conflict of Interest

The authors declare no conflict of interest.

Keywords

ionic circuit, ionic diode, LASER engraving, polyelectrolyte gel, stretchable diode

Received: September 30, 2018

Revised: November 18, 2018

Published online:

- [1] J.-Y. Sun, C. Keplinger, G. M. Whitesides, Z. Suo, *Adv. Mater.* **2014**, 26, 45.
- [2] C.-C. Kim, H.-H. Lee, K. H. Oh, J.-Y. Sun, *Science* **2016**, 353, 682.
- [3] M. S. Sarwar, Y. Dobashi, C. Preston, J. K. M. Wyss, S. Mirabbasi, J. D. W. Madden, *Sci. Adv.* **2017**, 3, e1602200.
- [4] C. Keplinger, J.-Y. Sun, C. C. Foo, P. Rothmund, G. M. Whitesides, Z. Suo, *Science* **2013**, 341, 984.
- [5] Y. Lee, S. H. Cha, Y.-W. Kim, D. Choi, J.-Y. Sun, *Nat. Commun.* **2018**, 9, 1804.
- [6] W. Xu, L.-B. Huang, M.-C. Wong, L. Chen, G. Bai, J. Hao, *Adv. Energy Mater.* **2017**, 7, 1.
- [7] T. B. H. Schroeder, A. Guha, A. Lamoureux, G. VanRenterghem, D. Sept, M. Shtein, J. Yang, M. Mayer, *Nature* **2017**, 552, 214.

- [8] O. J. Cayre, S. T. Chang, O. D. Velev, *J. Am. Chem. Soc.* **2007**, *129*, 10801.
- [9] J. H. Han, K. B. Kim, H. C. Kim, T. D. Chung, *Angew. Chem., Int. Ed.* **2009**, *48*, 21.
- [10] J. H. Han, K. B. Kim, J. H. Bae, B. J. Kim, C. M. Kang, H. C. Kim, H. C. Kim, T. D. Chung, *Small* **2011**, *7*, 8.
- [11] E. O. Gabrielson, P. Janson, K. Tybrandt, D. T. Simon, M. Berggren, *Adv. Mater.* **2014**, *26*, 5143.
- [12] S. H. Han, S.-R. Kwon, S. Baek, T.-D. Chung, *Sci. Rep.* **2017**, *7*, 1.
- [13] Y. Zhou, Y. Hou, Q. Li, L. Yang, Y. Cao, K. H. Choi, Q. Wang, Q. M. Zhang, *Adv. Mater. Technol.* **2017**, *2*, 9.
- [14] K. B. Kim, J.-H. Han, H. C. Kim, T. D. Chung, *Appl. Phys. Lett.* **2010**, *96*, 14.
- [15] K. Tybrandt, K. C. Larsson, A. Richter-Dahlfors, M. Berggren, *Proc. Natl. Acad. Sci. USA* **2010**, *107*, 9929.
- [16] K. Tybrandt, E. O. Gabrielson, M. Berggren, *J. Am. Chem. Soc.* **2011**, *133*, 10141.
- [17] K. Tybrandt, R. Forchheimer, M. Berggren, *Nat. Commun.* **2012**, *3*, 871.
- [18] G. Sun, S. Senapati, H.-C. Chang, *Lab Chip* **2016**, *16*, 7.
- [19] J. P. Gong, Y. Katsuyama, T. Kurokawa, Y. Osada, *Adv. Mater.* **2003**, *15*, 258.
- [20] H. J. Kwon, Y. Osada, J. P. Gong, *Polym. J.* **2006**, *38*, 1211.
- [21] J. P. Gong, *Soft Matter* **2010**, *6*, 12.
- [22] J. Duan, W. Xie, P. Yang, J. Li, G. Xue, Q. Chen, B. Yu, R. Liu, J. Zhou, *Nano Energy* **2018**, *48*, 569.
- [23] R. Skouri, F. Schosseler, J. P. Munch, S. J. Candau, *Macromolecules* **1995**, *28*, 197.
- [24] M. Rubinstein, R. H. Colby, A. V. Dobrynin, J.-F. Joanny, *Macromolecules* **1996**, *29*, 398.
- [25] S. Schneider, P. Linse, *Eur. Phys. J. I E* **2002**, *8*, 457.
- [26] W. Hong, X. Zhao, Z. Suo, *J. Mech. Phys. Solids* **2010**, *58*, 558.
- [27] H. Yuk, T. Zhang, G. A. Parada, X. Liu, X. Zhao, *Nat. Commun.* **2016**, *7*, 12028.
- [28] N. Lu, X. Wang, Z. Suo, J. Vlassak, *J. Mater. Res.* **2009**, *24*, 2.